Chiral Ferrocenyl–Iodotriazoles and –Iodotriazoliums as Halogen Bond Donors. Synthesis, Solid State Analysis and Catalytic Properties.

Emmanuel Aubert,[c] Abdelatif Doudouh,[c] Emmanuel Wenger,[c] Barbara Sechi,[b] Paola Peluso,*[b] Patrick Pale[a] and Victor Mamane*[a]

Dedication ((optional))

[a] Prof. Dr. P. Pale, Dr. V. Mamane
Institute of Chemistry of Strasbourg, UMR 7177 - LASYROC
CNRS and Strasbourg University
4 rue Blaise Pascal, 67000 Strasbourg, France
E-mail: vmamane@unistra.fr (VM); www.asymhole.cnrs.fr
[b] Dr. P. Peluso, B. Sechi
Istituto di Chimica Biomolecolare ICB
CNR, Sede secondaria di Sassari
Traversa La Crucca 3, Regione Baldinca, 07100 Li Punti, Sassari, Italy
E-mail: paola.peluso@cnr.it (PP)
[c] A. Doudouh, E. Wenger, Dr. E. Aubert
Université de Lorraine, CNRS, CRM2 , F-54000 Nancy, France

Supporting information for this article is given via a link at the end of the document.((Please delete this text if not appropriate))

Abstract: Despite the increasing number of applications based on halogen bond (XB), asymmetric catalysis purely based on such supramolecular interactions still remains a huge challenge. The first step toward its development is the design of appropriate XB chiral donor molecules with good catalytic properties. In this context, we report the synthesis of a series of iodinated compounds based on the triazole or triazolium ring and possessing the planar chirality of ferrocene. Their XB donor property was attested by X-ray diffraction analysis, showing short I•••N and I•••F interactions in the triazole-based derivatives and in the tetrafluoroborate salt of a idodotriazolium, respectively. The potential of these compounds to act as XB-based catalysts was demonstrated in the aza-Diels-Alder reaction involving an imine and a diene. Whereas triazole-based derivatives were inactive in this reaction, the triflate salts of iodotriazoliums delivered the expected cycloadduct with high yield.

Introduction

According to the IUPAC definition,[1] "a halogen bond occurs when there is evidence of a net attractive interaction between an electrophilic region associated with a halogen atom in a molecular entity and a nucleophilic region in another, or the same, molecular entity." The "electrophilic region" to which the definition refers corresponds to the σ-hole whose concept was introduced by Politzer and *coll.*.[2] This localized region of lower electrostatic potential is not limited to halogen and can be found in many other bonded atoms.[3]

Since the beginning of the 21st century, the halogen bond (XB) have gained more and more importance in the field of non-covalent interactions.[4] Indeed, an increasing number of applications based on XB have been reported in the literature in the last years. These applications are covering numerous fields such as polymer and material science,[5] separation science,[6] organic synthesis,[7] catalysis,[8] biological science,[9] anion recognition,[10] and crystal engineering.[11]

Iodotriazolium salts are known as strong XB donors because of the increasing effect on the iodine σ-hole depth provided by the positive charge borne by the heteroaromatic ring.[12] After their pioneering use in XB-based anion-binding rotaxanes,[13] these salts and their azolium analogues have become very popular in catalysis[8,14] and anion recognition.[15] Recently, structures based on the neutral iodotriazole unit have also found multiple applications.[16]

In general, iodotriazoles are obtained by [2+3] cycloaddition between iodoalkynes and alkyl or aryl azides.[17] However, most reported chiral iodotriazoles were produced from chiral azides,[18] derived either from natural substances (carbohydrates,[19] aminoacids,[20] alkaloids[21]) or from unnatural compounds, such as phenethylamine,[22] cyclohexyldiamine[16g] or BINOL[23]). In contrast, chiral iodotriazoles made from chiral alkynyl derivatives remained very scarce,[24] and none has been derived from planar chiral derivatives (Figure 1a).

These few chiral iodotriazoles and iodotriazolium salts, issued from chiral azides, showed interesting results in the enantiomeric discrimination of chiral molecules,[21b,23] but moderate[16g,25] or no chiral induction could be achieved when they were used as catalysts in various reactions.[22a-b] It is thus worth looking for new and improved chiral organocatalysts relying on iodotriazole and iodotriazolium entity, especially those in which chirality will be brought by the iodoalkyne moiety.

Currently developing new and efficient XB and chalcogen bond donors for catalysis applications,[26] we recently reported that chiral ferrocenyl iodoalkynes possess interesting XB properties in solid state and in solution, and exhibit promising catalytic properties, especially in Ritter reaction.[27] In the present

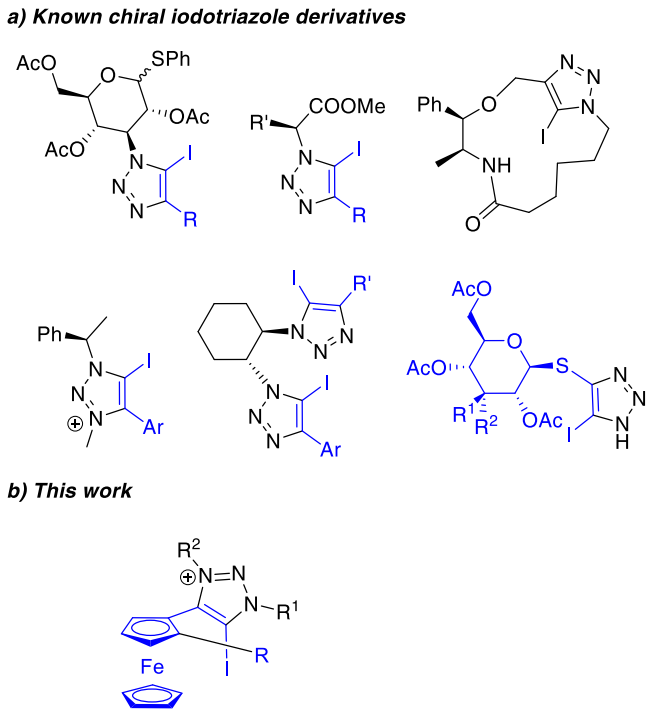

Figure 1. Known chiral iodotriazoles and those described in the present work.

work, we have taken benefit of this context to design, prepare and study new chiral derivatives in which chirality is brought by iodoalkynes bearing axially chiral 1,2- disubstituted ferrocenyl unit. It is worth noticing here that only a few works reported the synthesis of iodo-triazoles and -triazoliums bearing ferrocenyl moiety, but in achiral versions.[28]

Herein, enantiopure ferrocenyl iodotriazoles and iodotriazolium salts were prepared (Figure 1b). These new compounds were studied in the solid state through X-Ray Diffraction (XRD) and their catalytic properties were evaluated in the aza-Diels-Alder reaction.[29]

Results and Discussion

Synthesis.

Racemic and enantiopure ferrocenyl iodoalkynes **1**[27] were transformed in two steps, through iodotriazoles **2**, to the tetrafluoroborate triazolium salts **3(BF$_4$)** (Scheme 1). First, compounds **1** were reacted with benzyl azide in the presence of a catalytic amount of CuI and tris((1-benzyl-1*H*-1,2,3-triazolyl)methyl)amine (TBTA) in THF at room temperature.[30] The reaction proved to be very slow and full conversion could be obtained after 48h by raising the amount of the catalytic system from 5 to 15 mol%. Under these conditions, a series of triazole derivatives **2** (Table 1, fourth column) bearing halogen (F, Cl, Br, entries 1-4), methyl or cyano groups (entries 5 and 6), as well as aromatic rings (phenyl, 2-naphthyl, entries 7-9) were obtained with moderate to good yields. The high enantiomeric excess (ee) of the starting iodoalkynyl ferrocenes were preserved during these syntheses, as revealed by the measured ees for iodotriazoles *S*$_{Fc}$-**2c** and *S*$_{Fc}$-**2g** compared to parent iodoalkynes *S*$_{Fc}$-**1c** and *S*$_{Fc}$-**1g** (entries 4 and 9). Then, a selection of five ferrocenyltriazoles **2** comprising three racemic (entries 3, 7 and 8)

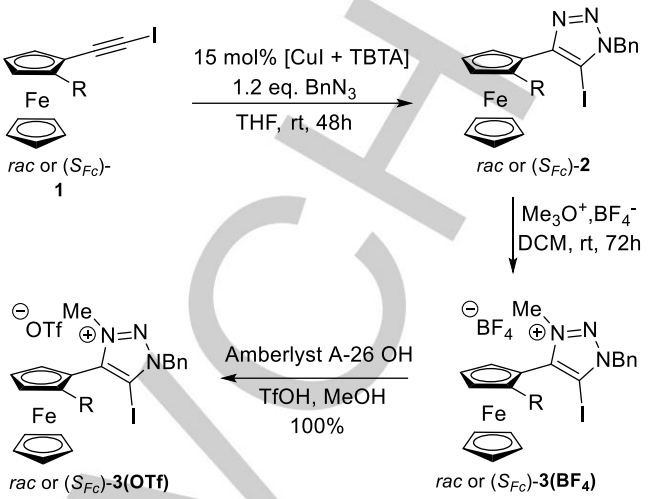

Scheme 1. Synthesis of ferrocenyl-based iodotriazoles **2** and iodotriazolium salts **3**.

and two enantiopure compounds (entries 4 and 9) were *N*-methylated by addition of the Meerwein salt (Me_3OBF_4) in dichloromethane (DCM) to give triazoliums salts **3(BF$_4$)** in good to high yields (Table 1, fifth column). Here again, the reaction was very slow and complete conversion was obtained after 72h in the dark. Finally, the BF_4^- anion could be quantitatively exchanged by TfO^- by using the freshly prepared Amberlyst OTf resin[31] (Table 1, sixth column), as shown by the preparation of triazoliums salts *rac*-**3f(OTf)** (entry 7) and *S*$_{Fc}$-**3g(OTf)** (entry 9). It is worth noting that the direct synthesis of *rac*-**3f(OTf)** from *rac*-**2f** by addition of MeOTf resulted in complete degradation.

Table 1. Synthetized products and corresponding yields.

Entry	R	**1**	**2**[a]	**3(BF$_4$)**[a]	**3(OTf)**[a]
1	F	*rac*-**1a**	*rac*-**2a** (66)	-	-
2	Cl	*rac*-**1b**	*rac*-**2b** (52)	-	-
3	Br	*rac*-**1c**	*rac*-**2c** (85)	*rac*-**3c(BF$_4$)** (63)	-
4	Br	*S*$_{Fc}$-**1c** (98.3% ee)	*S*$_{Fc}$-**2c** (80) (97.1% ee)	*S*$_{Fc}$-**3c(BF$_4$)** (73)	-
5	Me	*rac*-**1d**	*rac*-**2d** (51)	-	-
6	CN	*rac*-**1e**	*rac*-**2e** (94)	-	-
7	C_6H_5	*rac*-**1f**	*rac*-**2f** (84)	*rac*-**3f(BF$_4$)** (97)	*rac*-**3f(OTf)** (100)
8	β-Napht	*rac*-**1g**	*rac*-**2g** (77)	*rac*-**3g(BF$_4$)** (85)	-
9	β-Napht	*S*$_{Fc}$-**1g** (97.4 % ee)	*S*$_{Fc}$-**2g** (87) (98.2 % ee)	*S*$_{Fc}$-**3g(BF$_4$)** (67)	*S*$_{Fc}$-**3g(OTf)** (100)

[a] Yield (%) is given in brackets.

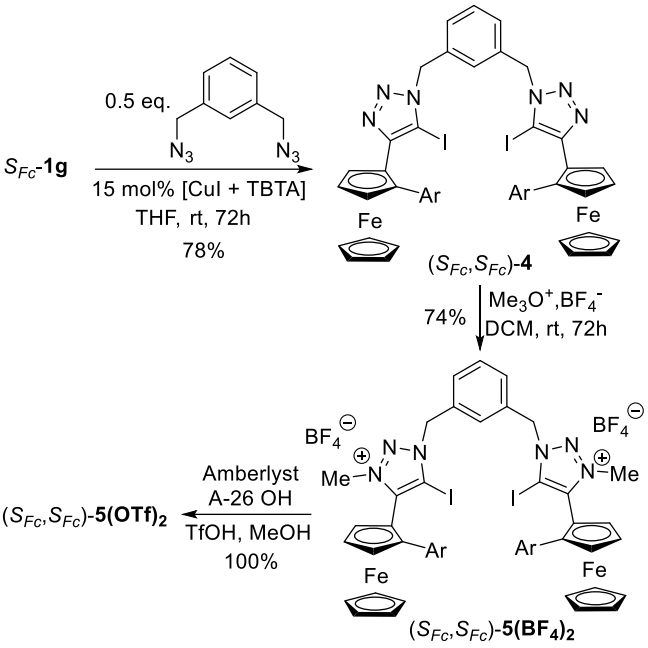

Scheme 2. Synthesis of enantiopure bidendate ferrocenyl-iodotriazole **4** and -iodotriazolium salts **5** (Ar = 2-naphthyl).

Given the importance of chelating XB donor molecules in molecular recognition and catalysis[8,10,16a-g,25] the chiral enantiopure bis-triazolium salts (S_{Fc}, S_{Fc})-**5(BF$_4$)$_2$** and (S_{Fc}, S_{Fc})-**5(OTf)$_2$** were prepared from S_{Fc}-**1g** by following the same chemical sequence comprising click reaction to give (S_{Fc}, S_{Fc})-**4**, *N*-methylation for the formation of (S_{Fc}, S_{Fc})-**5(BF$_4$)$_2$** and finally anionic exchange to produce (S_{Fc}, S_{Fc})-**5(OTf)$_2$** (Scheme 2). All these steps were very efficient, furnishing the bis-iodotriazolium salts with a very good overall yield of 58%.

X-Ray Diffraction Analysis.

Crystal structures of ferrocenyl–iodotriazoles *rac*-**2a**, *rac*-**2c**, *rac*-**2d** and *rac*-**2g** were determined by single crystal X-ray diffraction (XRD). All four ferrocenyl–iodotriazoles structures display infinite halogen bonded chains (Figure 2), with the σ-hole of the iodine atoms pointing toward the 3-N triazole nitrogen atoms (crystallographic labels N3 and N6, see Figures S1-S4 in S. I.) with almost linear C-I···N angles (Table 2).

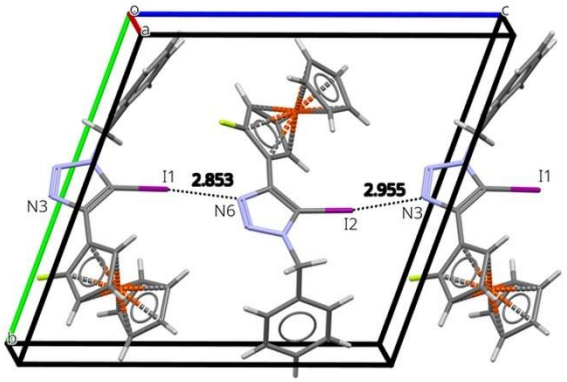

Figure 2. Infinite halogen bonded chain in the crystal structure of *rac*-**2a**. Interatomic distances given in Å. Only the major disorder component is shown.

Table 2. Geometrical contact characteristics of XBs observed between iodine and 3-N triazole nitrogen atoms.

Compound	d(I···N) (Å)	PP[a]	α(C-I···N) (°)
rac-**2a**	2.853 / 2.955	0.81 / 0.84	173.8 / 171.2
rac-**2c**	2.987	0.85	175.6
rac-**2d**	2.986	0.85	179.0
rac-**2g**	3.032	0.86	175.4

[a] Penetration parameter, defined as the ratio of the observed interatomic distance with respect to the sum of the corresponding van der Waals atomic radii (r_{vdw}(N) = 1.55 Å; r_{vdw}(I) = 1.98 Å).

In each case, the highest DFT computed electrostatic surface potential (ESP) maximum $V_{S,max}$ is located in the extension of the C-I bond (the σ-hole) and faces the most negative ESP which is located in proximity of the 3-N triazole nitrogen atom (Table S1 in S. I.). The magnitude of these ESP extrema varies on the *R* substituent, the shortest **I•••N** XB was observed being obtained for the ferrocenyl–iodotriazole *rac*-**2a** for which $|V_{S,max}-V_{S,min}|$ is the largest.

In all four ferrocenyl–iodotriazoles the computed molecular dipole moments are in the range 3.5-5.0 D and are oriented parallel to the 3-N triazole nitrogen to iodine atoms direction (Figures S13-S16 in S. I.). The observed molecular chains can then be described as head to tail alignment of these dipole moments; a Cambridge Structural Database search (see section 4 in S. I. for details) revealed that such a motif is common for iodotriazole containing molecules, where about one third of the structures display such halogen bonded motif (Table S2 in S. I.).

These C-I···N bonded chains are isolated in *rac*-**2g**, assembled in antiparallel pairs in *rac*-**2c** and *rac*-**2d** or forming planes in *rac*-**2a**, with numerous π-π and C-H···π contacts completing the 3D networking. In *rac*-**2c** the iodotriazole units of adjacent chains are on the top of each other (Figure 3), facing complementary atomic charges in a favourable way (Q(C-C-I) = +0.81|e|; Q(N-N-N) = -1.34|e|; Figure S17 in S. I.). In this particular compound, an additional σ-hole interaction involves the bromine substituent on cyclopentadiene (Cp) ring and the 2-N triazole

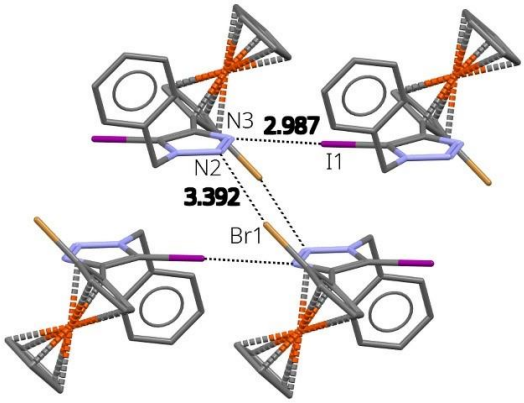

Figure 3. Interaction between adjacent infinite halogen bonded chains in the crystal structure of *rac*-**2c**. Interatomic distances given in Å. Only the major disorder component is shown. The C-I···N chains pairs up on top of each other in order to maximize favourable electrostatic interactions between positively charged CC-I and negatively charged N-N-N parts of iodotriazole moieties.

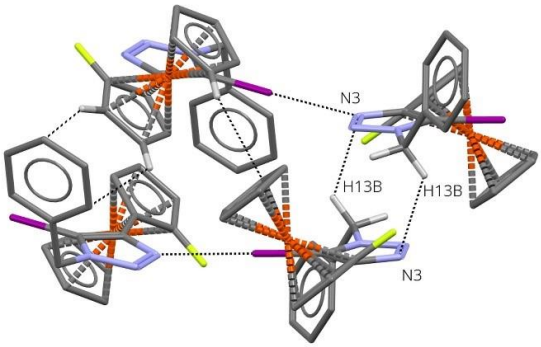

Figure 4. Interaction between adjacent infinite halogen bonded chains in the crystal structure of *rac*-**2a**. The C-I···N chains pairs up on top of each other in order to maximize favourable electrostatic interactions between positively charged CH_2 groups and negatively charged N-N-N parts of iodotriazole moieties.

nitrogen atom (C-Br1···N2 = 3.392 Å, PP = 1.00, 147.98°), although this interaction is weak due to deactivation of the halogen atom which is bonded to a cyclopentadienyl ring (Q(Br) = -0.05|e|; ESP on prolongation of C-Br: $V_{S,max}$ = 4.81 kcal/mol; $V_{S,min}$(2-N) = -32.17 kcal/mol).

Compound *rac*-**2d** being isostructural with *rac*-**2c**, the same crystal packing is then observed. The bromine atom is here replaced by a methyl group which is approximately oriented toward the same nucleophilic area (C-$C6_{Me}$···N2 = 3.461 Å; 144.71°). Nevertheless, the methyl group is not activated due to its bonding to the Cp ring, as revealed by the lack of an extremum in the prolongation of the C-C_{Me} bond in the DFT calculated ESP surface. Therefore, a tetrel bond cannot be invoked here.

In *rac*-**2a** the C-I···N bonded chains interact closely together making infinite (010) planes, where the electropositive region about the CH_2 group (Figure 4; $V_{S,max}$ = 19.15 to 23.82 kcal/mole) faces electronegative area about the 3-N atom of triazole moiety. These differences in crystal packing can be related to the different conformations adopted between the triazole ring and the ferrocenyl moiety. Whereas the iodine atom lies in between the Cp rings of the adjacent ferrocenyl in *rac*-**2a** (Figures 2 and 4; Fe1-C1-C11-I1 = -54.08°/Fe2-C20-C30-I2 = -60.28°; see Figures S1-S4 in S. I. for atom labelling), the C-I bond is oriented toward the exterior of the molecule in *rac*-**2c,d** (Figure 3; Fe1-C1-C11-I1 = -135.24° and Fe1-C1-C12-I1 = -132.28°) and is even almost perpendicular to the Cp in *rac*-**2g** (Fe1-C1-C11-I1 = 179.25°), leading also to different relative orientation of the Cp *R* substituent relative to the iodotriazole plane.

Crystal structure of *rac*-**3f(BF4)** was also determined by single crystal XRD. The methylation of nitrogen 3-N, which is the σ-hole acceptor in the neutral structures, and the presence of BF_4^- counter ion break the formation of the previously reported C-I···N halogen bonded chains. Indeed, the iodine σ-hole (Figure S12 in S. I.) is directed toward one fluorine atom of a BF_4^- anion (C44-I2···F1 = 2.918Å; PP = 0.85; 166.68°; C18-I1···F7 = 3.067Å; PP = 0.89; 160.49°). However, the area above and below the triazole ring is slightly more electropositive ($V_{S,max}$(triazole) = 101.02 kcal/mole > $V_{S,max}$(I) = 97.30 kcal/mol; see Figure S12 in S. I.) and the anion is also interacting with these most electropositive regions of the cation (Figure 5), avoiding contact with the π clouds of Ph and Cp rings of the cation which are the least electropositive areas.

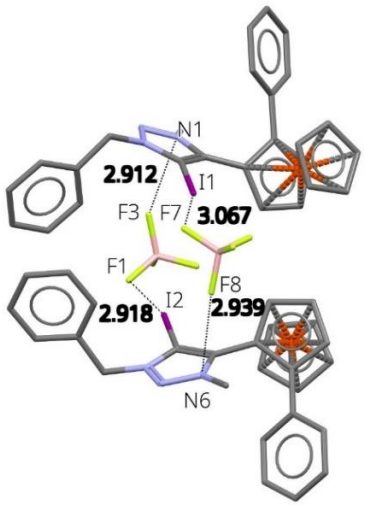

Figure 5. Packing of BF_4^- anions and iodotriazolium cations in *rac*-**3f(BF4)**. Hydrogen atoms and CH_2Cl_2 molecule are omitted for clarity. Selected interatomic distances are given in Å.

Organocatalysis.

In order to study the catalytic activity of the synthesized XB donors, the aza-Diels-Alder reaction between Danishefsky's diene **6** and imines **7** was selected (Table 3). Indeed, this reaction was already described to be catalyzed by different XB donors,[26c,32] including triazolium salts.[22b,33]

Table 3. XB-Catalyzed Aza Diels-Alder reaction

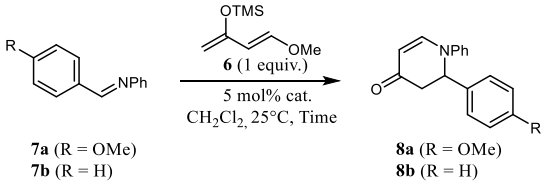

7a (R = OMe)
7b (R = H)

8a (R = OMe)
8b (R = H)

Entry	Imine	Catalyst	Time	Conversion (%)[a]	ee (%)[f]
1	**7a**	*rac*-**1f**	24h	0	-
2	**7a**	*rac*-**2f**	24h	0	-
3	**7a**	*rac*-**3c(BF$_4$)**	24h	0	-
4	**7a**	*rac*-**3f(OTf)**	6h	100 (89%)	-
5[b]	**7a**	*rac*-**3f(OTf)**	6h	100 (94%)	-
6[c]	**7a**	*rac*-**3f(OTf)**	6h	0	-
7[d]	**7a**	*rac*-**3f(OTf)**	6h	0	-
8	**7b**	*rac*-**3f(OTf)**	6h	100 (92%)	-
9	**7a**	S_{Fc}-**3g(OTf)**	6h	100 (92%)	0
10[e]	**7a**	(S_{Fc},S_{Fc})-**4**	24h	7	n.d.[g]
11[e]	**7a**	(S_{Fc},S_{Fc})-**5(OTf)$_2$**	4h	100 (96%)	6.4

[a] Yield (%) of **8** is given in brackets; [b] with 10 mol% K_2CO_3; [c] with 5 mol% of *n*-Bu$_4$NCl; [d] with 5 mol% of TBAOTf; [e] 2.5 mol% catalyst were used; [f] ee% determined by enantioselective HPLC (Lux Amylose-1); [g] n.d.: not determined.

The role the nature of the backbone carrying the iodine atom could play was first analyzed by comparing iodoalkyne *rac*-**1f**, triazole *rac*-**2f**, and triazolium salts *rac*-**3f(BF$_4$)** and *rac*-**3f(OTf)** in the aza-Diels-Alder reaction between diene **6** and imine **7a** in dichloromethane at room temperature (entries1-4). Although it could promote the Ritter reaction,[27] *rac*-**1f** remained inactive in this reaction since no conversion was observed after 24h of reaction (entry 1). Similarly, its triazolyl derivative *rac*-**2f** did not give any conversion, although a strong XB was observed in the corresponding solid (entry 2). As the solid shows strong intermolecular XB between the iodine of one molecule and the N-3 of triazole of the next molecule, the same XB may persist in solution and thus compete with the N atom of the imine. Therefore, the latter could not be activated and no reaction occurred. Surprisingly, the corresponding triazolium *rac*-**3f(BF$_4$)** was also inactive in this reaction, despite the presence of the charge-activated iodine σ-hole and the absence of the N3 lone pair (entry 3).[22c] Gratifyingly, *rac*-**3f(OTf)** could efficiently catalyze the reaction, affording complete conversion to adduct **8a** after 6h at 25°C (entry 4). This large counterion effect, and in particular the ineffectiveness of the BF_4 salts, was recently highlighted in the context of σ-hole-based catalysis.[22b,31,34] This lack of catalytic activity was imputed to the lower stability of the tetrafluoroborate salts in the reaction mixture. Complete conversion was also obtained by addition of K_2CO_3 in the reaction mixture containing catalyst *rac*-**3f(OTf)** (entry 5); this result ruled out the catalytic role of possible residual trifluoromethanesulfonic acid used during the anionic exchange step.

Addition of tetrabutylammonium chloride (TBACl) as a source of chloride anion acting as substrate competitor toward the catalyst completely inhibited the reaction, confirming that halogen bonding is indeed involved in the catalysis (entry 6). Moreover, tetrabutylammonium triflate (TBAOTf) was inactive in the reaction (entry 7) indicating that the triflate anion did not play a role in the catalytic activity of *rac*-**3f(OTf)**. A possible charge transfer mechanism[26c] with the iodotriazolium moiety was also ruled out by using imine **7b** without the *p*-methoxy substituent; the latter was indeed completely converted to adduct **8b** after 6h at 25°C as efficiently as its methoxylated analog **7a** (entry 8 vs 4). The enantiopure catalyst S_{Fc}-**3g(OTf)** delivered the expected product with complete conversion and high yield but as a racemic mixture (entry 9). With a potentially chelating structure, the bis-iodotriazole **4** was expected to be more reactive and more able to induce enantioselectivity in its enantiopure form. The latter (S_{Fc},S_{Fc})-**4** was thus submitted to imine **7a** under the same conditions as above. A very low conversion could be achieved, while the monomeric analog *rac*-**2f** did not provide any transformation (entry 10 vs 2). Nevertheless, this result confirmed the very low or lack of activity of iodotriazole-based catalysts in this reaction. As in the monomeric series, the corresponding bis-triazolium triflate (S_{Fc},S_{Fc})-**5(OTf)$_2$** showed a sharp reactivity increase, allowing complete conversion and high yield after 4h of reaction (entry 11). Providing the expected adduct in slightly higher yield (96 vs 91%) within shorter reaction time (4h vs 6h), such bis-iodotriazolium is thus more efficient catalyst than its monomeric analog (entry 11 vs 4). It is worth noticing that these results favorably compared to those already reported. Indeed, when using an analog iodoimidazolium as catalyst at the same loading, Minakata and *coll.* obtained the same adduct with a lower 57% yield.[32] With a related iodotriazolium, Kanger and *coll.* achieved 95% conversion after 6h but with a 20 mol% catalyst loading.[22b] Furthermore, some enantioselectivity was also observed during the reaction, as revealed by the adduct ee. This result confirmed the beneficial role of having two iodotriazole motifs in the catalyst structure. The low obtained value may be due to the relative flexibility of the bridging motif employed here. It is nevertheless encouraging and improvement can be expected by optimizing the reaction condition and/or by increasing the rigidity of the catalysts.

Conclusion

A new family of chiral XB donors was prepared, analyzed in the solid state and evaluated in catalysis. These compounds are based on: i) iodine as the σ-hole donor atom, ii) the triazolium ring to increase the σ-hole depth, and iii) a disubstituted ferrocene as the chiral source. In the solid state, the triazoles and triazoliums derivatives display clear evidence of molecular organization driven by the halogen σ-hole. Good catalytic activity was observed at room temperature with the iodotriazolium triflates in an aza-Diels- Alder reaction, and the best performance was achieved with a bidendate derivative. Currently, only low asymmetric induction was observed during the reaction with an enantiopure bidendate catalyst. This encouraging results motivate us to further develop this new family of chiral XB-based catalysts; work is thus in progress in our laboratory in order to modify the structure of these promising catalysts and to test them in other catalytic reaction.

Experimental Section

General Information. Proton (^{1}H NMR), fluorine (^{19}F NMR) and carbon (^{13}C NMR) nuclear magnetic resonance spectra were recorded on the following 300, 400, or 500 MHz instruments. The chemical shifts are given in parts per million (ppm) on the delta scale. The solvent peak was used as reference values. For ^{1}H NMR: $CDCl_3$ = 7.26 ppm, CD_2Cl_2 = 5.32 ppm. For ^{13}C NMR: $CDCl_3$ = 77.16 ppm, CD_2Cl_2 = 53.84 ppm. Data are

presented as follows: chemical shift, multiplicity (s = singlet, d = doublet, t = triplet, q = quartet, quint = quintet, m = multiplet, b = broad), integration, and coupling constants (*J*/Hz). High-resolution mass spectra (HRMS) data were recorded on a micrOTOF spectrometer equipped with an orthogonal electrospray interface (ESI). $[\alpha]_D$ values were measured at the sodium D-line on a JASCO J-815 CD spectropolarimeter, in $CHCl_3$ in a quartz cuvette (1 cm) at 20°C. Melting points were obtained in open capillary tubes and are uncorrected. Analytical thin layer chromatography (TLC) was carried out on silica gel 60 F254 plates with visualization by ultraviolet light. Reagents and solvents were purified using standard means. Tetrahydrofuran (THF) was distilled from sodium metal/benzophenone and used freshly. Anhydrous dichloromethane (DCM) and methanol were obtained by passing through activated alumina under a positive pressure of argon using GlassTechnology GTS100 devices. Anhydrous reactions were carried out in flame-dried glassware and under an argon atmosphere. All other chemicals were used as received. Compounds **1** were prepared according to literature procedures.[27]

General procedure for the [2+3] cycloaddition reaction. CuI (15 mol% relative to **1**) and TBTA (15 mol% relative to **1**) were dissolved in THF (0.2 M) and the mixture was stirred for 30 min at room temperature. A THF solution (1 M) of BnN_3 (1.2 eq. relative to **1**) or 1,3-bis(azidomethyl)benzene (0.5 eq. relative to S_{Fc}-**1g**) was added followed by the ferrocenyl iodoalkyne derivative **1** which is added as a solid. The mixture was stirred at room temperature for 48h in the dark. DCM was added (20 mL/mmol) and the mixture was washed with a solution of NH_4OH (2x10 mL/mmol). The organic phase was dried over $MgSO_4$, filtered and concentrated. The product was purified by chromatography on silica gel (pentane/ethyl acetate mixture).

(*rac*)-1-Benzyl-4-(2-fluoroferrocenyl)-5-iodo-1*H*-1,2,3-triazole (*rac*-2a). Orange solid (30 mg, 66%) obtained from *rac*-**1a** (0.093 mmol, 33 mg). Mp: 158-160°C. ^{1}H NMR (500 MHz, $CDCl_3$) δ 7.28-7.41 (m, 5H), 5.65 (s, 2H), 4.49 (m, 2H), 4.30 (s, 5H), 3.97 (m, 1H); ^{13}C NMR (126 MHz, $CDCl_3$) δ 148.0 (d, J_{F-C} = 5.0 Hz), 135.5, 134.3, 129.0, 128.6, 128.0, 77.5, 71.0, 63.7 (d, J_{F-C} = 10.1 Hz), 62.0 (d, J_{F-C} = 2.5 Hz), 60.9 (d, J_{F-C} = 3.8 Hz), 56.9 (d, J_{F-C} = 15.1 Hz), 54.5; ^{19}F NMR (282 MHz, $CDCl_3$) δ -184.1. HRMS (ESI-TOF) *m/z* $[M]^+$ Calcd for $C_{19}H_{15}FFeIN_3$ 486.9639; Found 486.9641.

(*rac*)-1-Benzyl-4-(2-chloroferrocenyl)-5-iodo-1*H*-1,2,3-triazole (*rac*-2b). Orange solid (15 mg, 52%) obtained from *rac*-**1b** (0.057 mmol, 21 mg). Mp: 161-163°C. ^{1}H NMR (500 MHz, $CDCl_3$) δ 7.30-7.41 (m, 5H), 5.63 (s, 2H), 4.57 (dd, *J* = 2.5, 1.5 Hz, 1H), 4.53 (dd, *J* = 2.5, 1.5 Hz, 1H), 4.35 (s, 5H), 4.21 (t, *J* = 2.5 Hz, 1H); ^{13}C NMR (126 MHz, $CDCl_3$) δ 148.0, 134.5, 129.0, 128.6, 128.1, 92.4, 80.1, 74.2, 72.0, 68.9, 67.6, 65.8, 54.5. HRMS (ESI-TOF) *m/z* $[M]^+$ Calcd for $C_{19}H_{15}ClFeIN_3$ 502.9343; Found 502.9341.

(*rac*)-1-Benzyl-4-(2-bromoferrocenyl)-5-iodo-1*H*-1,2,3-triazole (*rac*-2c). Orange solid (93 mg, 85%) obtained from *rac*-**1c** (0.2 mmol, 83 mg). Mp: 168-170°C. ^{1}H NMR (500 MHz, $CDCl_3$) δ 7.41-7.30 (m, 5H), 5.65 (d, *J* = 15.5 Hz, 1H), 5.61 (d, *J* = 15.5 Hz, 1H), 4.60 (dd, *J* = 2.5, 1.5 Hz, 1H), 4.54 (dd, *J* = 2.5, 1.5 Hz, 1H), 4.36 (s, 5H), 4.27 (t, *J* = 2.5 Hz, 1H); ^{13}C NMR (126 MHz, $CDCl_3$) δ 148.3, 134.5, 129.0, 128.6, 128.1, 80.6, 78.8, 72.4, 71.3, 68.4, 67.2, 54.5. HRMS (ESI-TOF) *m/z* $[M]^+$ Calcd for $C_{19}H_{15}BrFeIN_3$ 546.8838; Found 546.8833.

(S_{Fc})-1-Benzyl-4-(2-bromoferrocenyl)-5-iodo-1*H*-1,2,3-triazole (S_{Fc}-2c). Orange solid (60 mg, 80%) obtained from S_{Fc}-**1b** (0.137 mmol, 58 mg). Mp: 123-125°C. $[\alpha]_D$ = +109° (c 0.93, $CHCl_3$); HRMS (ESI-TOF) *m/z* $[M]^+$ Calcd for $C_{19}H_{15}BrFeIN_3$ 546.8838; Found 546.8845.

(*rac*)-1-Benzyl-4-(2-methylferrocenyl)-5-iodo-1*H*-1,2,3-triazole (*rac*-2d). Orange solid (42 mg, 51%) obtained from *rac*-**1d** (0.169 mmol, 59 mg). Mp: 138-140°C. ^{1}H NMR (500 MHz, $CDCl_3$) δ 7.42-7.28 (m, 5H), 5.64 (d, *J* = 15.0 Hz, 1H), 5.60 (d, *J* = 15.0 Hz, 1H), 4.67 (dd, *J* = 2.5, 1.5 Hz, 1H), 4.25 (dd, *J* = 2.5, 1.5 Hz, 1H), 4.17 (t, *J* = 2.5 Hz, 1H), 4.14 (s, 5H), 2.30 (s, 3H); ^{13}C NMR (126 MHz, $CDCl_3$) δ 150.3, 134.6, 129.0, 128.5, 127.9, 84.4, 77.9, 74.6, 70.6, 70.3, 67.8, 66.7, 54.3, 14.9. HRMS (ESI-TOF) *m/z* $[M]^+$ Calcd for $C_{20}H_{18}FeIN_3$ 482.9889; Found 482.9896.

(*rac*)-1-Benzyl-4-(2-cyanoferrocenyl)-5-iodo-1*H*-1,2,3-triazole (*rac*-2e). Orange solid (36 mg, 94%) obtained from *rac*-**1e** (0.078 mmol, 28 mg). Mp: 40-42°C. ^{1}H NMR (500 MHz, $CDCl_3$) δ 7.42-7.29 (m, 5H), 7.65 (d, *J* = 15.5 Hz, 1H), 7.62 (d, *J* = 15.5 Hz, 1H), 4.95 (dd, *J* = 3.0, 1.5 Hz, 1H), 4.82 (dd, *J* = 3.0, 1.5 Hz, 1H), 4.54 (t, *J* = 3.0, 1H), 4.40 (s, 5H); ^{13}C NMR (126 MHz, $CDCl_3$) δ 147.2, 134.2, 129.1, 128.7, 128.1, 119.8, 78.6, 78.4, 72.9, 72.3, 70.9, 70.8, 54.6, 52.7. HRMS (ESI-TOF) *m/z* $[MH]^+$ Calcd for $C_{20}H_{16}FeIN_4$ 494.9764; Found 494.9759.

(*rac*)-1-Benzyl-4-(2-phenylferrocenyl)-5-iodo-1*H*-1,2,3-triazole (*rac*-2f). Orange solid (177 mg, 84%) obtained from *rac*-**1f** (0.388 mmol, 160 mg). Mp: 142-144°C. ^{1}H NMR (500 MHz, $CDCl_3$) δ 7.39-7.30, 7.22 (d, *J* = 6 Hz, 2H), 7.16 (t, *J* = 3.5 Hz, 3H), 5.59 (d, *J* = 15.5 Hz, 1H), 5.54 (d, *J* = 15.5 Hz, 1H), 4.63 (dd, *J* = 2.5, 1.5 Hz, 1H), 4.58 (dd, *J* = 2.5, 1.5 Hz, 1H), 4.42 (t, *J* = 2.5 Hz, 1H), 4.29 (s, 5H); ^{13}C NMR (126 MHz, $CDCl_3$) δ 149.9, 138.4, 134.7, 129.0, 128.9, 128.5, 128.0, 127.7, 126.3, 87.7, 82.0, 75.7, 71.5, 71.2, 68.6, 68.1, 54.4. HRMS (ESI-TOF) *m/z* $[M]^+$ Calcd for $C_{25}H_{20}FeIN_3$ 545.0046; Found 545.0042.

(*rac*)-1-Benzyl-4-[2-(naphthalen-2-yl)ferrocenyl)]-5-iodo-1*H*-1,2,3-triazole (*rac*-2g). Orange solid (74 mg, 77%) obtained from *rac*-**1g** (0.162 mmol, 75 mg). Mp: 167-169°C. ^{1}H NMR (500 MHz, $CDCl_3$) δ 7.76 (dd, *J* = 6.0, 3.0 Hz, 1H), 7.73 (br s, 1H), 7.63 (dd, *J* = 6.0, 3.0 Hz, 1H), 7.61 (d, *J* = 8.5 Hz, 1H), 7.46 (dd, *J* = 8.5, 2.0 Hz, 1H), 7.44-7.39 (m, 2H), 7.36-7.30 (m, 3H), 7.24-7.19 (m, 2H), 5.59 (d, *J* = 15.5 Hz, 1H), 5.52 (d, *J* = 15.5 Hz, 1H), 4.75 (dd, *J* = 3.0, 1.5 Hz, 1H), 4.63 (dd, *J* = 3.0, 1.5 Hz, 1H), 4.47 (t, *J* = 3.0 Hz, 1H), 4.32 (s, 5H); ^{13}C NMR (126 MHz, $CDCl_3$) δ 150.0, 136.2, 134.7, 133.4, 132.2, 129.0, 128.5, 127.8, 127.75, 127.74, 127.0, 87.4, 82.1, 76.0, 71.8, 71.2, 68.6, 68.3, 54.4. HRMS (ESI-TOF) *m/z* $[M]^+$ Calcd for $C_{29}H_{22}FeIN_3$ 595.0202; Found 595.0209.

(S_{Fc})-1-Benzyl-4-[2-(naphthalen-2-yl)ferrocenyl)]-5-iodo-1*H*-1,2,3-triazole S_{Fc}-2g). Orange solid (52 mg, 87%) obtained from S_{Fc}-**1g** (0.1 mmol, 46 mg). Mp: 121-123°C. $[\alpha]_D$ = –172° (c 0.76, $CHCl_3$); HRMS (ESI-TOF) *m/z* $[M]^+$ Calcd for $C_{29}H_{22}FeIN_3$ 595.0203; Found 595.0212.

(S_{Fc},S_{Fc})-1,3-Bis[(5-iodo-4-(2-(naphthalen-2-yl)ferrocenyl)-1H-1,2,3-triazol-1-yl)methyl]benzene ((S_{Fc},S_{Fc})-4). Orange solid (87 mg, 78%) obtained from S_{Fc}-**1g** (0.2 mmol, 92.4 mg). Mp: 143-145°C. $[\alpha]_D$ = –142° (c 0.64, $CHCl_3$); ^{1}H NMR (500 MHz, $CDCl_3$) δ 7.77-7.69 (m, 4H), 7.64-7.55 (m, 4H), 7.47 (dd, *J* = 8.5, 2.0 Hz, 2H), 7.42-7.36 (m, 4H), 7.29 (t, *J* = 7.5 Hz, 1H), 7.15 (dd, *J* = 8.5, 2.0 Hz, 2H), 7.08 (s, 1H), 5.50 (d, *J* = 15.5 Hz, 2H), 5.40 (d, *J* = 15.5 Hz, 2H), 4.73 (dd, *J* = 3.0, 1.5 Hz, 2H), 4.57 (dd, *J* = 3.0, 1.5 Hz, 2H), 4.45 (t, *J* = 3.0 Hz, 2H), 4.30 (s, 10H); ^{13}C NMR (126 MHz, $CDCl_3$) δ 150.0, 136.1, 135.3, 133.4, 132.2, 129.6, 127.8, 127.7, 127.3, 127.2, 126.9, 126.1, 125.6, 87.4, 82.1, 75.8, 71.8, 71.2, 68.6, 68.4, 54.1. HRMS (ESI-TOF) *m/z* $[M]^+$ Calcd for $C_{52}H_{38}Fe_2I_2N_6$ 1111.9941; Found 1111.9945.

General procedure for the *N*-methylation. To a solution of **2** in DCM (0.1 M) at room temperature was added Me_3O^+,BF_4^- and the mixture was stirred for 72h in the dark. MeOH was added (2 mL/mmol) and the solution was concentrated. The crude was dissolved in DCM (4 mL/mmol) and the product was precipitated by addition of diethyl ether (100 mL/mmol). The powder was filtered, washed with diethyl ether (50 mL/mmol) and dried under vacuum for 1 day. Note: two peaks with approximatively 3:1 ratio were observed for the BF_4 anion in the ^{19}F NMR spectrum of all prepared salts. It is probably the result of the slow displacement (in the NMR timescale) of BF_4 anion between the *N*-Me and *N*-Bn positive charge in the triazolium ring.

(*rac*)-1-Benzyl-5-iodo-3-methyl-4-(2-bromoferrocenyl)-1H-1,2,3-triazol-3-ium tetrafluoroborate (*rac*-3c(BF_4)). Orange solid (43 mg, 63%) obtained from *rac*-**2c** (0.11 mmol, 60 mg). Mp: 102-104°C. ^{1}H NMR (500 MHz, CD_2Cl_2) δ 7.60-7.40 (m, 5H), 5.84 (d, *J* = 15.0 Hz, 1H), 5.80 (d,

J = 15.0 Hz, 1H), 4.86 (s, 1H), 4.77 (s, 1H), 4.68 (s, 1H), 4.54 (s, 5H), 4.43 (broad s, 3H); ^{13}C NMR (126 MHz, CD_2Cl_2) δ 145.7, 131.1, 130.2, 129.8, 129.5, 79.5, 73.4, 73.3, 70.2, 69.8, 69.2, 59.2, 40.9; ^{19}F NMR (282 MHz, CD_2Cl_2) δ -153.36, -153.41. HRMS (ESI-TOF) *m/z* $[M]^+$ Calcd for $C_{20}H_{18}BrFeIN_3$ 561.9073; Found 561.9081; *m/z* $[M]^-$ Calcd for BF_4 87.0035; Found 87.0029.

(*S*$_{Fc}$)-1-Benzyl-5-iodo-3-methyl-4-(2-bromoferrocenyl)-1H-1,2,3-triazol-3-ium tetrafluoroborate (*S*$_{Fc}$-3c(BF$_4$)). Orange solid (25 mg, 73%) obtained from *S*$_{Fc}$-**2c** (0.055 mmol, 30 mg). Mp: 111-113°C. $[\alpha]_D$ = –19° (c 1.64, $CHCl_3$). HRMS (ESI-TOF) *m/z* $[M]^+$ Calcd for $C_{20}H_{18}BrFeIN_3$ 561.9074; Found 561.9060; *m/z* $[M]^-$ Calcd for BF_4 87.0035; Found 87.0032.

(*rac*)-1-Benzyl-5-iodo-3-methyl-4-(2-phenylferrocenyl)-1H-1,2,3-triazol-3-ium tetrafluoroborate (*rac*-3f(BF$_4$)). Orange solid (60 mg, 97%) obtained from *rac*-**2f** (0.1 mmol, 54.5 mg). Mp: 127-129°C. ^{1}H NMR (500 MHz, CD_2Cl_2) δ 7.60-7.35 (m, 5H), 7.35-7.07 (m, 5H), 5.78 (s, 2H), 5.00 (s, 1H), 4.86 (s, 1H), 4.79 (s, 1H), 4.45 (s, 5H), 3.94 (broad s, 3H); ^{13}C NMR (126 MHz, CD_2Cl_2) δ 147.3, 136.7, 131.3, 130.2, 129.8, 129.4, 129.3, 128.9, 128.2, 88.4, 72.7, 72.3, 71.9, 71.5, 67.4, 59.0, 40.1; ^{19}F NMR (282 MHz, CD_2Cl_2) δ -153.33, -153.39. HRMS (ESI-TOF) *m/z* $[M]^+$ Calcd for $C_{26}H_{23}FeIN_3$ 560.0281; Found 560.0248; *m/z* $[M]^-$ Calcd for BF_4 87.0035; Found 87.0034.

(*rac*)-1-Benzyl-5-iodo-3-methyl-4-[2-(naphthalen-2-yl)ferrocenyl]-1H-1,2,3-triazol-3-ium tetrafluoroborate (*rac*-3g(BF$_4$)). Orange solid (87 mg, 85%) obtained from *rac*-**2g** (0.165 mmol, 90 mg). Mp: 162-164°C. ^{1}H NMR (500 MHz, CD_2Cl_2) δ 7.86-7.80 (m, 1H), 7.78 (d, *J* = 8.5 Hz, 1H), 7.74-7.69 (m, 1H), 7.65 (s, 1H), 7.55-7.38 (m, 7H), 7.36 (d, *J* = 8.5 Hz, 1H), 5.79 (s, 2H), 5.10 (s, 1H), 4.87 (s, 1H), 4.83 (s, 1H), 4.44 (s, 5H), 3.99 (broad s, 3H); ^{13}C NMR (126 MHz, CD_2Cl_2) δ 147.4, 134.4, 133.8, 133.0, 131.4, 130.1, 129.8, 129.3, 129.2, 128.2, 128.1, 127.3, 127.0, 126.9, 126.8, 88.3, 73.6, 72.5, 71.7, 71.6, 67.4, 59.5, 40.2; ^{19}F NMR (282 MHz, CD_2Cl_2) δ -152.95, -153.00. HRMS (ESI-TOF) *m/z* $[M]^+$ Calcd for $C_{30}H_{25}FeIN_3$ 610.0437; Found 610.0471; *m/z* $[M]^-$ Calcd for BF_4 87.0035; Found 87.0031.

(*S*$_{Fc}$)-1-Benzyl-5-iodo-3-methyl-4-[2-(naphthalen-2-yl)ferrocenyl]-1H-1,2,3-triazol-3-ium tetrafluoroborate (*S*$_{Fc}$-3g(BF$_4$)). Orange solid (25 mg, 67%) obtained from *S*$_{Fc}$-**2g** (0.05 mmol, 30 mg). Mp: 185-187°C. HRMS (ESI-TOF) *m/z* $[M]^+$ Calcd for $C_{30}H_{25}FeIN_3$ 610.0437; Found 610.0454; *m/z* $[M]^-$ Calcd for BF_4 87.0035; Found 87.0039.

(*S*$_{Fc}$,*S*$_{Fc}$)-1,1'-[1,3-Phenylenebis(methylene)bis(5-iodo-3-methyl-4-(2-(naphthalen-2-yl)ferrocenyl)-1*H*-1,2,3-triazol-3-ium] bis-tetrafluoroborate ((*S*$_{Fc}$,*S*$_{Fc}$)-5(BF$_4$)$_2$). Orange solid (49 mg, 74%) obtained from *S*$_{Fc}$-**2g** (0.05 mmol, 55.6 mg). Mp: 178-180°C. $[\alpha]_D$ = –77° (c 0.30, $CHCl_3$); ^{1}H NMR (500 MHz, CD_2Cl_2) δ 7.88-7.68 (m, 8H), 7.61 (s, 1H), 7.56-7.41 (m, 7H), 7.38 (d, *J* = 8.5 Hz, 2H), 5.78 (d, *J* = 15.5 Hz, 2H), 5.75 (d, *J* = 15.5 Hz, 2H), 5.07 (s, 2H), 4.86 (s, 2H), 4.79 (s, 2H), 4.41 (s, 10H), 3.97 (broad s, 6H); ^{13}C NMR (126 MHz, CD_2Cl_2) δ 147.4, 134.5, 133.8, 133.0, 132.2, 130.7, 130.5, 129.1, 128.3, 128.1, 127.2, 127.1, 127.0, 126.8, 88.7, 88.4, 72.6, 71.6, 71.5, 67.5, 58.6, 40.2; ^{19}F NMR (282 MHz, CD_2Cl_2) δ -152.09, -152.15. HRMS (ESI-TOF) *m/z* $[M]^{2+}$ Calcd for $C_{54}H_{44}Fe_2I_2N_6$ 571.0202; Found 571.0203; *m/z* $[M]^-$ Calcd for BF_4 87.0035; Found 87.0034.

General procedure for the anion exchange.[31] Amberlyst® A26 (OH) (1 gram per 100 mg of *rac*-**3f(BF$_4$)** and *S*$_{Fc}$-**3g(BF$_4$)** and 1 gram per 50 mg of **((***S*$_{Fc}$, *S*$_{Fc}$)-**5(BF$_4$)$_2$)** was suspended in methanol (10 mL per gram resin), carefully stirred and cooled to 0 °C. After 15 minutes, trifluoromethanesulfonic acid (20.0 mmol per gram resin) was added dropwise over a period of 10 minutes. The mixture was carefully stirred for 30 minutes at 0 °C and then poured into a thin glass column and rinsed with methanol until a neutral pH was obtained. Subsequently, the BF_4 salt dissolved in methanol (0.05 M) was poured onto the column and rinsed slowly through the column. The collected solution was rinsed two more times through the column and finally the column was rinsed with methanol (50 mL per gram resin). The solvent was removed under reduced pressure and the residue dried under high vacuum to obtain the triflate salt.

(*rac*)-1-Benzyl-5-iodo-3-methyl-4-(2-phenylferrocenyl)-1H-1,2,3-triazol-3-ium trifluoromethanesulfonate (*rac*-3f(OTf)). Orange solid (77 mg, 100%) obtained from *rac*-**3f(BF$_4$)** (0.113 mmol, 70 mg). Mp: 92-94°C. ^{1}H NMR (500 MHz, CD_2Cl_2) δ 7.45 (s, 5H), 7.16-7.35 (m, 5H), 5.78 (s, 2H), 4.97 (s, 1H), 4.85 (s, 1H), 4.76 (s, 1H), 4.43 (s, 5H), 3.88 (broad s, 3H); ^{13}C NMR (126 MHz, CD_2Cl_2) δ 147.2, 136.7, 131.4, 130.1, 129.7, 129.4, 128.8, 128.1, 121.6 (q, *J* = 322.6 Hz, CF_3), 89.9, 89.3, 72.6, 72.4, 71.7, 71.4, 67.5, 59.0, 40.0; ^{19}F NMR (282 MHz, CD_2Cl_2) δ -78.5. HRMS (ESI-TOF) *m/z* $[M]^+$ Calcd for $C_{26}H_{23}FeIN_3$ 560.0281; Found 560.0299; *m/z* $[M]^-$ Calcd for CF_3O_3S 148.9526; Found 148.9523.

(*S*$_{Fc}$)-1-Benzyl-5-iodo-3-methyl-4-(2-(naphthalen-2-yl)ferrocenyl)-1H-1,2,3-triazol-3-ium trifluoromethanesulfonate (*S*$_{Fc}$-3g(OTf)). Orange solid (23 mg, 100%) obtained from *S*$_{Fc}$-**3g(BF$_4$)** (0.027 mmol, 21 mg). Mp: 100-102°C. $[\alpha]_D$ = –64° (c 0.81, $CHCl_3$). ^{1}H NMR (500 MHz, $CDCl_3$) δ 7.86-7.74 (m, 2H), 7.72-7.65 (m, 2H), 7.62 (s, 1H), 7.52-7.32 (m, 8H), 5.81 (s, 2H), 5.01 (s, 1H), 4.96 (s, 1H), 4.75 (s, 1H), 4.45 (s, 5H), 3.87 (broad s, 3H); ^{13}C NMR (126 MHz, $CDCl_3$) δ 146.7, 134.3, 133.4, 132.6, 131.3, 129.8, 129.5, 129.1, 129.05, 128.0, 127.8, 127.1, 126.6, 126.5, 126.4, 120.8 (q, *J* = 321.3 Hz, CF_3), 89.2, 88.0, 72.8, 72.5, 71.1, 70.7, 67.6, 58.7, 39.9; ^{19}F NMR (282 MHz, $CDCl_3$) δ -78.3. HRMS (ESI-TOF) *m/z* $[M]^+$ Calcd for $C_{30}H_{25}FeIN_3$ 610.0437; Found 610.0424; *m/z* $[M]^-$ Calcd for CF_3O_3S 148.9526; Found 148.9524.

(*S*$_{Fc}$, *S*$_{Fc}$)-1,1'-(1,3-Phenylenebis(methylene))bis(5-iodo-3-methyl-4-(2-(naphthalen-2-yl)ferrocenyl)-1*H*-1,2,3-triazol-3-ium) bis-trifluoromethanesulfonate ((*S*$_{Fc}$, *S*$_{Fc}$)-5(OTf)$_2$). Orange solid (27 mg, 100%) obtained from (*S*$_{Fc}$, *S*$_{Fc}$)-**5(BF$_4$)$_2$** (0.019 mmol, 25 mg). Mp: 193-195°C. $[\alpha]_D$ = –45° (c 0.74, $CHCl_3$); ^{1}H NMR (500 MHz, CD_2Cl_2) δ 7.90-7.72 (m, 7H), 7.70 (s, 2H), 7.57-7.42 (m, 7H), 7.31 (d, *J* = 8.5 Hz, 2H), 5.80 (s, 4H), 5.12 (s, 2H), 4.92 (s, 2H), 4.81 (s, 2H), 4.48 (s, 10H), 3.87 (broad s, 6H); ^{13}C NMR (126 MHz, CD_2Cl_2) δ 147.4, 134.5, 133.7, 133.0, 132.2, 131.2, 130.7, 130.5, 129.1, 128.2, 128.1, 127.1, 127.0, 126.9, 126.8, 121.4 (q, *J* = 352.8 Hz, CF_3), 90.0, 89.0, 72.9, 71.8, 71.6, 67.7, 58.5, 40.2; ^{19}F NMR (282 MHz, CD_2Cl_2) δ -78.5. HRMS (ESI-TOF) *m/z* $[M]^{2+}$ Calcd for $C_{54}H_{44}Fe_2I_2N_6$ 571.0204; Found 571.0177; *m/z* $[M]^-$ Calcd for CF_3O_3S 148.9526; Found 148.9524.

General procedure for the aza Diels-Alder reaction. In a round-bottom flask under argon at 25°C, the imine (0.1 mmol) and the catalyst (0.05 mmol or 0.025 mmol in case of chelating catalysts) were diluted in dry CH_2Cl_2 (0.5 mL). *Trans*-1-methoxy-3-trimethylsiloxy-1,3-butadiene (0.12 mmol, 25 μL) was added and the mixture was stirred for a period of time. The reaction was quenched by addition of 0.5 mL of TBAF (1.0 M in THF) and the mixture was stirred for 15 min. Water (2 mL) and CH_2Cl_2 (2 mL) was added and the phases were separated. The aqueous phase was extracted with CH_2Cl_2 (2×2 mL) then the organic phases were combined and dried over $MgSO_4$. After filtration and concentration, the crude was purified by chromatography on silica gel (cyclohexane / ethyl acetate 1 / 1) to give pure product.

X-ray Diffraction Analysis. Single crystals of *rac*-**2a** and *rac*-**3f(BF$_4$)** were obtained from by slow evaporation from an *n*-hexane/dichloromethane 1/1 solution. *Rac*-**2c** single crystals were obtained by slow evaporation from an ethanol solution. Single crystal of *rac*-**2d** (resp. *rac*-**2g**) were obtained by slow cooling (from 60°C to 20°C at a rate of 0.1°C/mn) of a saturated solution in methanol (resp. acetonitrile) using a MW96 multiwall apparatus from Anacristmat (http://www.anacrismat.com/). Data for compounds *rac*-**2a** (CCDC 2115921)**,** *rac*-**2c** (CCDC 2115923)**,** *rac*-**2d** (CCDC 2115920) and *rac*-**2g** (CCDC 2115922) were collected on SuperNova diffractometer using the Mo(Kα) radiation at low temperature using a nitrogen cold stream (T=100 K). Data for compounds *rac*-**3f(BF$_4$)** (CCDC 2114936) were collected on a Bruker D8 Venture DUO diffractometer with a PHOTON III CPAD detector equipped with an Oxford Cryosystem liquid N_2 device,

using the Mo(Kα) radiation at low temperature using a nitrogen cold stream (T=120 K).

Acknowledgements

This work was supported by the CNRS, University of Strasbourg and by French National Research Agency (ANR-21-CE07-0014). “The Plateforme de Mesures de Diffraction et Diffusion des rayons X (PMD2X) of Université de Lorraine” is thanked for providing access to crystallographic facilities. The EXPLOR mesocentre is thanked for computing facilities (Project 2019CPMXX0984).

Keywords: Catalysis • Chirality • Ferrocene • Halogen Bond • Triazolium

[1] G. R. Desiraju, P. S. Ho, L. Kloo, A. C. Legon, R. Marquardt, P. Metrangolo, P. Politzer, G. Resnati, K. Rissanen, *Pure Appl. Chem.* **2013**, *85*, 1711–1713.

[2] a) T. Brinck, J. S. Murray, P. Politzer, *Int. J. Quantum Chem.* **1992**, *44*, 57–64; b) P. Politzer, P. Lane, M. C. Concha, Y. Ma, J. S. Murray, *J. Mol. Model.* **2007**, *13*, 305–311.

[3] J. S. Murray, P. Lane, P. Politzer, *J. Mol. Model.* **2009**, *15*, 723–729.

[4] G. Cavallo, P. Metrangolo, R. Milani, T. Pilati, A. Priimagi, G. Resnati, G. Terraneo, *Chem. Rev.* **2016**, *116*, 2478–2601.

[5] a) R. Kampes, S. Zechel, M. D. Hager, U. S. Schubert, *Chem. Sci.* **2021**, *12*, 9275–9286; b) S. Biswas, A. Das, *ChemNanoMat* **2021**, *7*, 748–772; c) D. Devadiga, T. N. Ahipa, *J. Mol. Liq.* **2021**, *333*, 115961; d) W. Wang, Y. Zhang, W. J. Jin, *Coord. Chem. Rev.* **2020**, *404*, 213107.

[6] a) P. Peluso, V. Mamane, A. Dessì, R. Dallocchio, E. Aubert, C. Gatti, D. Mangelings, S. Cossu, *J. Chromatogr. A* **2020**, *1616*, 460788; b) P. Peluso, V. Mamane, R. Dallocchio, A. Dessì, R. Villano, D. Sanna, E. Aubert, P. Pale, S. Cossu, *J. Sep. Sci.* **2018**, *41*, 1247–1256; c) R. Dallocchio, A. Dessì, M. Solinas, A. Arras, S. Cossu, E. Aubert, V. Mamane, P. Peluso, *J. Chromatogr. A* **2018**, *1563*, 71–81.

[7] a) W. Lorpaiboon, P. Bovonsombat, *Org. Biomol. Chem.* **2021**, 10.1039/d1ob00936b; b) S. Yamada, T. Konno, *Curr. Org. Chem.* **2020**, *14*, 2118–215.

[8] a) M. Kaasik, T. Kanger, *Front. Chem.* **2020**, *8*, 599064; b) M. Breugst, J. J. Koenig, *Eur. J. Org. Chem.* **2020**, 5473–5487; c) R. Sutar, S. M. Huber, *ACS Catal.* **2019**, *9*, 9622–9639; d) J. Bamberger, F. Ostler, O. Garcia Mancheño, *ChemCatChem* **2019**, *11*, 5198–5211.

[9] a) E. S. Marsan, C. A. Bayse, *Molecules* **2020**, *25*, 1328; b) V. Govindaraj, H. Ungati, S. R. Jakka, S. Bose, G. Mugesh, *Chem. Eur. J.* **2019**, *25*, 11180–11192; c) A. Dessì, P. Peluso, R. Dallocchio, R. Weiss, G. Andreotti, M. Allocca, E. Aubert, P. Pale, V. Mamane, S. Cossu, *Molecules* **2020**, *25*, 2213.

[10] a) M. S. Taylor, *Coord. Chem. Rev.* **2020**, *413*, 213270; b) J. Pancholi, P. D. Beer, *Coord. Chem. Rev.* **2020**, *416*, 213281.

[11] J. Teyssandier, K. S. Mali, S. De Feyter, *ChemistryOpen* **2020**, *9*, 225–241.

[12] A. Dreger, E. Engelage, B. Mallick, P. D. Beer, S. M. Huber, *Chem. Commun.* **2018**, *54*, 4013–4016.

[13] N. L. Kilah, M. D. Wise, C. J. Serpell, A. L. Thompson, N. G. White, K. E. Christensen, P. D. Beer, *J. Am. Chem. Soc.* **2010**, *132*, 11893–11895.

[14] Y. Kobayashi, Y. Takemoto, *Synlett* **2020**, *31*, 772–783.

[15] M. Foyle, N. G. White, *Chem. Asian J.* **2021**, *16*, 575–587.

[16] a) A. Docker, C. H. Guthrie, H. Kuhn, P. D. Beer, *Angew. Chem. Int. Ed.* **2021**, 10.1002/anie.202108591; b) A. Docker, X. Shang, D. Yuan, H. Kuhn, Z. Zhang, J. J. Davis, P. D. Beer, M. J. Langton, *Angew. Chem. Int. Ed.* **2021**, *60*, 19442–19450; c) G. Turner, A. Docker, P. D. Beer, *Dalton Trans.* **2021**, 10.1039/d1dt02414k; d) L. E. Bickerton, A. Docker, A. J. Sterling, H. Kuhn, F. Duarte, P. D. Beer, M. J. Langton, *Chem. Eur. J.* **2021**, *27*, 11738–11745; e) S. C. Patrick, R. Hein, A. Docker, P. D. Beer, J. J. Davis, *Chem. Eur. J.* **2021**, *27*, 10201–10209; f) Y. Cheong Tse, A. Docker, Z. Zhang, P. D. Beer, *Chem. Commun*. **2021**, *57*, 4950–4953; g) F. Ostler, D. G. Piekarski, T. Danelzik, M. S. Taylor, O. García Mancheño, *Chem. Eur. J.* **2021**, *27*, 2315–2320; h) R. Hein, X. Li, P. D. Beer, J. J. Davis, *Chem. Sci.* **2021**, *12*, 2433–2440; i) L. E. Bickerton, A. J. Sterling, P. D. Beer, F. Duarte, M. J. Langton, *Chem. Sci.* **2020**, *11*, 4722–4729.

[17] S. J. Gharpure, S. Naveen, R. S. Chavan, Padmaja, *Eur. J. Org. Chem.* **2020**, 6870–6886.

[18] M. Kaasik, S. Kaabel, K. Kriis, I. Jarving, T. Kanger, *Synthesis* **2019**, *51*, 2128−2135.

[19] a) L. Li, G. Zhang, A. Zhu, L. Zhan, *J. Org. Chem.* **2008**, *73*, 3630–3633; b) V. Malnuit, M. Duca, A. Manout, K. Bougrin, R. Benhida, *Synlett* **2009**, *13*, 2123–2126; c) D. Goyard, A. S. Chajistamatiou, A. I. Sotiropoulou, E. D. Chrysina, J-P. Praly, S. Vidal, *Chem. Eur. J.* **2014**, *20*, 5423–5432.

[20] O. J. Ingham, R. M. Paranal, W. B. Smith, R. A. Escobar, H. Yueh, T. Snyder, J. A. Porco, J. E. Bradner, A. B. Beeler, *ACS Med. Chem. Lett.* **2016**, *7*, 929–932.

[21] a) A. R. Bogdan, K. James, *Org. Lett.* **2011**, *13*, 4060–4063; b) M. Kaasik, S. Kaabel, K. Kriis, I. Jarving, R. Aav, K. Rissanen, T. Kanger, *Chem. Eur. J.* **2017**, *23*, 7337−7344.

[22] a) F. Kniep, L. Rout, S. M. Walter, H. K. V. Bensch, S. H. Jungbauer, E. Herdtweck, S. M. Huber, *Chem. Commun.* **2012**, *48*, 9299–9301; b) M. Kaasik, A. Metsala, S. Kaabel, K. Kriis, I. Järving, T. Kanger, *J. Org. Chem.* **2019**, *84*, 4294–4303; c) A. Peterson, M. Kaasik, A. Metsala, I. Jarving, J. Adamson, T. Kanger, *RSC Adv.* **2019**, *9*, 11718−11721.

[23] a) A. Borissov, J. Y. C. Lim, A. Brown, K. Christensen, A. L. Thompson, M. D. Smith, P. D. Beer, *Chem. Commun.* **2017**, *53*, 2483−2486; b) J. Y. C. Lim, I. Marques, V. Felix, P. D. Beer, *J. Am. Chem. Soc.* **2017**, 139, 12228–12239; c) J. Y. C. Lim, I. Marques, V. Félix, P. D. Beer, *Angew. Chem. Int. Ed.* **2017**, *57*, 584–588.

[24] J. C. Morris, J. Chiche, C. Grellier, M. Lopez, L. F. Bornaghi, A. Maresca, C.T. Supuran, J. Pouyssegur, S. A. Poulsen, *J. Med. Chem.* **2011**, *54*, 6905–6918.

[25] For a recent example using a chiral enantiopure bis(iodo-imidazolium) catalyst, see: R. L. Sutar, E. Engelage, R. Stoll, S. M. Huber, *Angew. Chem. Int. Ed.* **2020**, *59*, 6806−6810.

[26] R. Weiss, E. Aubert, P. Peluso, S. Cossu, P. Pale, V. Mamane, *Molecules* **2019**, *24*, 4484; b) R. Weiss, E. Aubert, P. Pale, V. Mamane, *Angew. Chem. Int. Ed.* **2021**, 60, 19281–19286; *Angew. Chem.* **2021**, *133*, 19430–19435; c) R. Weiss, T. Golisano, P. Pale, V. Mamane, *Adv. Synth. Catal.* **2021**, 363, 4779–4788.

[27] V. Mamane, P. Peluso, E. Aubert, R. Weiss, E. Wenger, S. Cossu, P. Pale, *Organometallics* **2020**, *39*, 3936–3950.

[28] a) J. Y. C. Lim, P. D. Beer, *Eur. J. Inorg. Chem.* **2017**, 220–224; b) F. Zapata, A. Caballero, P. Molina, *Eur. J. Inorg. Chem.* **2017**, 237–241; c) J. Y. C. Lim, M. J. Cunningham, J. J. Davis, P. D. Beer, *Chem. Commun.* **2015**, *51*, 14640–14643; d) J. Y. C. Lim, I. Marques, L. Ferreira, V. Félix, P. D. Beer, *Chem. Commun.* **2016**, *52*, 5527–5530; e) L. Gonzalez, F. Zapata, A. Caballero, P. Molina, C. Ramirez de Arellano, I. Alkorta, J. Elguero, *Chem. Eur. J.* **2016**, *22*, 7533–7544.

[29] G. Blond, M. Gulea, V. Mamane, *Curr. Org. Chem.* **2016**, *20*, 2161–2210.

[30] a) T. R. Chan; R. Hilgraf; K. B. Sharpless, V. V. Fokin, *Org. Lett.* **2004**, 6, 2853–2855; b) J. E. Hein, J. C. Tripp, L. B. Krasnova, K. B. Sharpless, V. V. Fokin, *Angew. Chem. Int. Ed.* **2009**, *48*, 8018–8021.

[31] T. Steinke, P. Wonner, E. Engelage, S. Huber, *Synthesis* **2021**, *53*, 2043–2050.

[32] Y. Takeda, D. Hisakuni, C H. Lin, S. Minakata, *Org. Lett.* **2015**, *17*, 318–321.

[33] R. Haraguchi, S. Hoshino, M. Sakai, S.-g. Tanazawa, Y. Morita, T. Komatsu, S.-i. Fukuzawa, *Chem. Commun.* **2018**, *54*, 10320–10323.

[34] X. He, X. Wang, Y.-L. S. Tse, Z. Ke, Y.-Y. Yeung, *ACS Catal.* **2021**, *11*, 12632–12642.

Entry for the Table of Contents

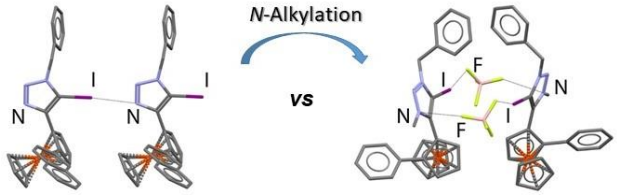

Planar chiral ferrocenyl halogen-bond donors with excellent catalytic properties are reported. Despite their propensity to form halogen-bonds in the solid state, the ferrocenyl iodotriazole derivatives were inactive as catalysts. Alkylation of the triazole ring afforded triazolium salts where iodine σ-hole depth was strongly increased, allowing efficient catalysis of an aza-Diels-Alder reaction through halogen-bond activation of the imine.

Institute and/or researcher Twitter usernames: @mamane_victor